

Supplementary Material

Table S1. Simulation results of $[Y(H_2O)_8]^{3+}$ clusters in the gas phase and similar clusters with a polarizable continuum (PC): Symmetry of the clusters, number of negative frequencies, geometrical parameters of the clusters, the electronic energies calculated. The data for the ν_1 Y-O breathing mode is also given for these DFT clusters.

Level of theory / basis set	symmetry	negative frequencies	ν_1 / cm^{-1} *	Y-O / Å	O-H / Å	H-O-H / °	energy in hartree
gas phase cluster							
B3LYP/LANL2DZ	C2	none	336.6	2.399	0.981	109.6	-648.698328
B3LYP/LANL2DZ	S8	none	336.5	2.399	0.981	109.6	-648.698322
B3LYP/LANL2DZ	D4	1	(334.2)	2.409	0.981	109.1	-648.688320
B3LYP/LANL2DZ/6-31G	C2	none	338.3	2.396	0.979	109.6	-648.511648
B3LYP/LANL2DZ/6-31G(d)	C2	none	328.4	2.408	0.977	106.0	-648.591925
B3LYP/LANL2DZ/6-1G+(d,p)	C2	none	338.3	2.396	0.978	109.6	-648.511648
B3LYP/LANL2DZ/D95+*	C2	none	334.0	2.414	0.978	105.9	-648.799550
B3LYP/LANL2DZ/D95**	C2	none	324.7	2.413	0.975	105.9	-648.848420
B3LYP/LANL2DZ/D95+**	C2	none	331.8	2.416	0.975	105.7	-648.864907
Cluster with PCM							
B3LYP/LANL2DZ	S8	none	372.1	2.354	0.989	110.9	-649.355492
B3LYP/LANL2DZ/6-31G+(d,p)	C2	-	no result	-	-	-	-
B3LYP/LANL2DZ/6-31G	C2	-	no result	-	-	-	-

- Remark: For the $[Y(H_2O)_8]^{3+}$ cluster with its 25 atoms $3 \times 25 - 6 = 69$ normal modes are expected with the irreducible representation of the normal modes: $\Gamma_{\nu}(S_8) = 8a(\text{Ra}) + 9b(\text{i.r.}) + 18e_1(\text{i.r.}) + 18e_2(\text{Ra}) + 16e_3(\text{Ra})$. The mode ν_1 is the totally symmetric Y-O mode, the so called breathing mode.

Table S2. Simulation results of a $[Y(H_2O)_6]^{3+}$ gas phase cluster and a similar clusters with a polarizable continuum (PCM). The symmetry of the cluster is T_h in both states. Given are frequency for the ν_1 Y-O breathing, the geometrical parameters of the cluster and the calculated electronic energy.

Level of theory / basis set	$\nu_1 / \text{cm}^{-1} *$	Y-O / Å	O-H / Å	H-O-H / °	Energy in hartree
B3LYP/LANL2DZ	376.5	2.322	0.986	107.8	-495.741633
B3LYP/LANL2DZ + PCM	407.5	2.285	0.986	109.4	-496.332300

- The mode ν_1 is the totally symmetric mode of Y-O (breathing mode).

Table S3: DFT frequencies at the B3LYP/ LANL2DZ level of theory for $[Y(H_2O)_8]^{3+}$ with a solvation shell (PC model). The irreducible representation of vibrations leads to $\Gamma_v(S_8) = 8a$ (Ra) + 9b (i.r.) + 18e₁ (Ra, i.r.) + 18e₂ (Ra) + 16e₃ (Ra).

peak position cm ⁻¹	sym- metry	assignment	peak position cm ⁻¹	sym- metry	assignment
27.1	e₂	δ YO₈	425.8	e ₁	ω H ₂ O
101.1	b	δ YO₈	523.0	b	ρ H ₂ O
109.3	e₁	δ YO₈	538.6	a	ρ H ₂ O
136.4	b	δ YO₈	566.0	e ₁	ρ H ₂ O
141.1	a	δ YO₈	566.2	e ₃	ρ H ₂ O
154.8	e₁	δ YO₈	594.7	e ₂	ρ H ₂ O
154.9	e₃	δ YO₈	1570.3	e ₂	δ H ₂ O
163.0	e₂	δ YO₈	1575.3	e ₃	δ H ₂ O
215.5	e ₂	τ H ₂ O	1580.0	e ₁	δ H ₂ O
250.0	e ₁	τ H ₂ O	1581.2	b	δ H ₂ O
278.8	e ₃	τ H ₂ O	1589.6	a	δ H ₂ O
283.6	e₂	v YO₈	3453.4	e ₂	v _s H ₂ O
301.3	e₃	v YO₈, τ H₂O	3454.0	e ₃	v _s H ₂ O
314.7	a	τH ₂ O	3456.9	b	v _s H ₂ O
336.7	b	v YO₈, ω H₂O	3459.6	e ₁	v _s H ₂ O
348.5	e₁	v YO₈, ω H₂O	3476.5	a	v _s H ₂ O
367.0	b	τH ₂ O, ω H ₂ O	3548.1	a	v _{as} H ₂ O
372.1	a	v_s YO₈	3548.3	e ₁	v _{as} H ₂ O
375.7	e ₃	ω H ₂ O	3548.3	e ₃	v _{as} H ₂ O
376.4	a	ω H ₂ O	3548.3	e ₂	v _{as} H ₂ O
384.8	b	ω H ₂ O	3548.5	b	v _{as} H ₂ O
397.6	e ₂	ω H ₂ O			

Note, that the skeletal vibrations are written in bold type letters, with the breathing vibrational frequency of the cluster at 372.1cm⁻¹. Notations: v_{as}: antisymmetric stretch, v_s: symmetric stretch, δ: deformation; H₂O librations: ρ: rocking, ω: wagging, τ: twisting

Table S4. Our Raman data and band assignments of CF_3SO_3^- (aq) at 23 °C.

Raman					assignment
peak position/ cm^{-1}	A_i	fwhh / cm^{-1}	depol. degree	symmetry	
-	-	-	-	a_2	torsion
212	0.97	18.1	0.65	e	$\tau_3\text{FC- SO}_3$
319	40.81	12.85	0.25	a_1	$\nu\text{ C-S}$
351	21.30	14.7	0.70	e	$\tau_3\text{FC- SO}_3$
518.8	1.97	16.1	0.64	e	$\delta_s\text{ FCF} + \delta_s\text{ SO}_3$
577.9	14.61	17.7	0.74	e	$\delta_{as}\text{ FCF}, \delta_{as}\text{ OSO}$
640.5	0.78	25.9	0.240	a_1	$\delta_{as}\text{ CF}_3, \delta_{as}\text{ OSO}$
764.5	48.05	8.45	0.0023	a_1	$\delta_s\text{ CF}_3, \delta_s\text{ SO}_3$
1033.3	100	12.9	0.0097	a_1	$\nu_s\text{ SO}_3, \nu_s\text{ CF}_3$
1182	2.33	27.8	0.71	e	$\nu_{as}\text{ CF}_3$
1227.5	4.54	9.8	0.21	a_1	$\nu_s\text{ CF}_3$
1254.5 *	2.38	46	0.63	e	$\nu_{as}\text{ SO}_3$
1281.8	15.79	33	0.70		

- This band appears as a double band; data from band fit procedure

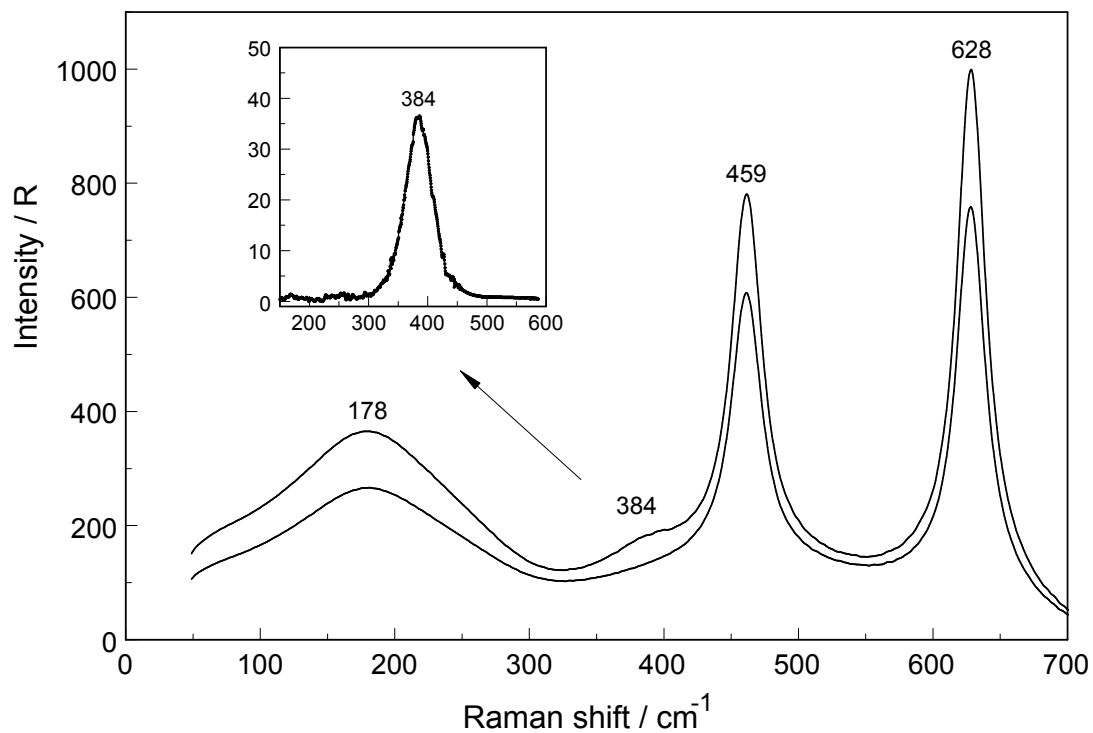


Figure S1. Polarized and depolarized Raman scattering profiles of $0.256 \text{ mol}\cdot\text{L}^{-1} \text{ Y}(\text{ClO}_4)_3(\text{aq})$ ($R_w = 211$). A. The inset shows the isotropic profile of the YO_8 breathing mode at 384 cm^{-1} ($R_{\text{iso}} = R_{\text{VV}} - 4/3R_{\text{VH}}$).

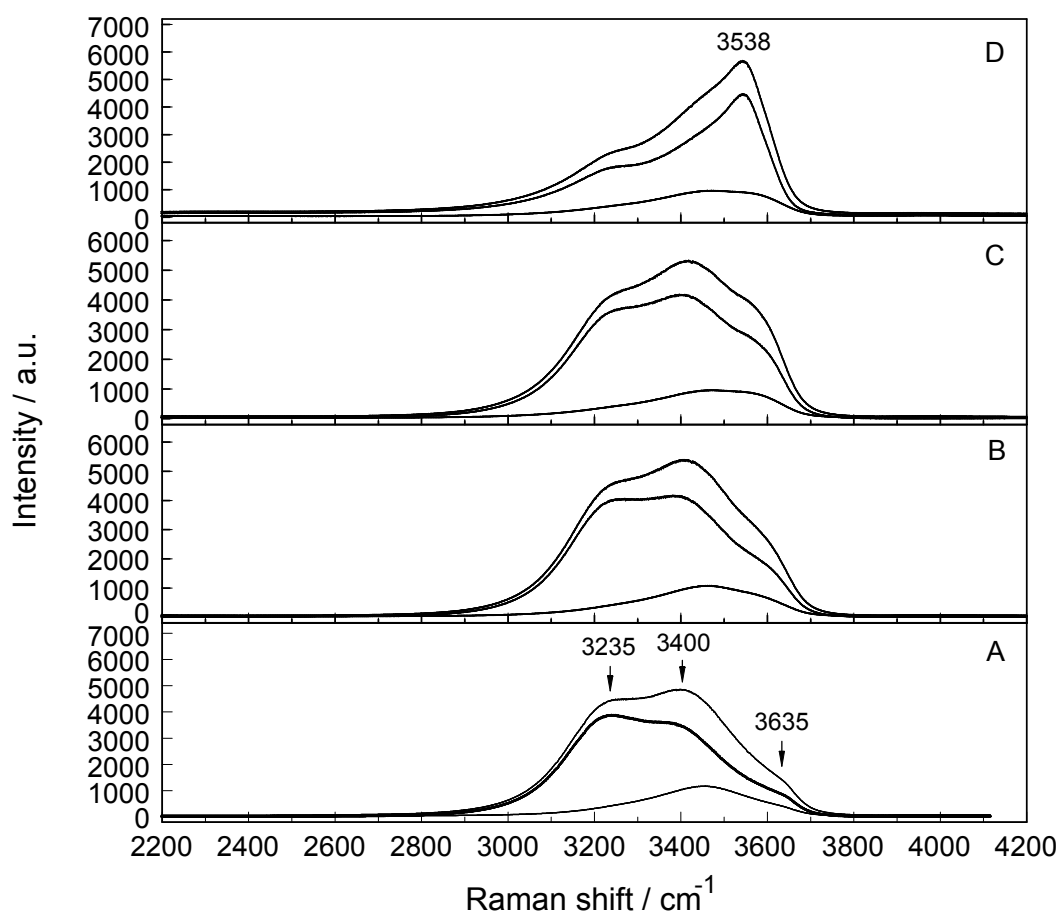


Figure S2. The O-H stretching region of water from 2200 – 4200 cm^{-1} for three aqueous $\text{Y}(\text{ClO}_4)_3$ solutions in comparison with neat liquid water. From bottom to top: (A) H_2O , (B) 0.390, (C) 0.76 and (D) 1.770 molL^{-1} $\text{Y}(\text{ClO}_4)_3$. At the bottom (A) the O-H profile of water with its characteristic bands is shown and above (B-D) the profiles of $\text{Y}(\text{ClO}_4)_3(\text{aq})$. With increasing solute concentration a mode at 3538 cm^{-1} is dominating the O-H profiles. (D) The band component of water at 3235 cm^{-1} is still observable while the component at 3405 cm^{-1} is completely overlapped by the strong band, ν O-H \cdots ClO_4^- , at 3538 cm^{-1} of weakly H-bonded water.

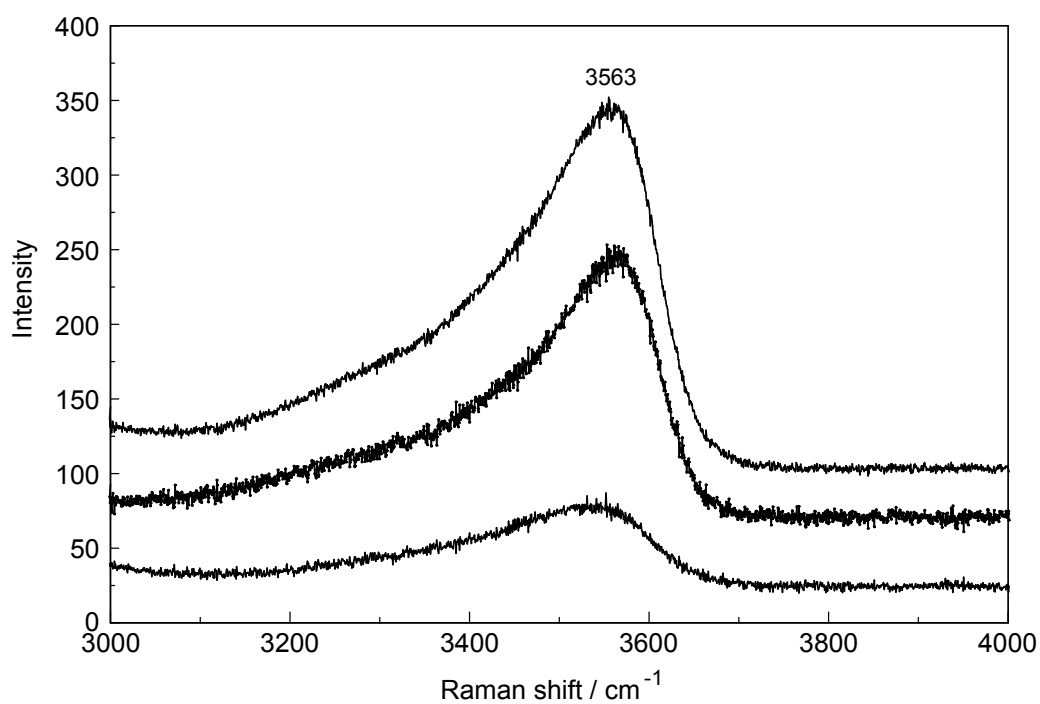


Figure S3. The O-H stretching region (HDO/D₂O; ca. 3% HDO) of a 2.300 mol L⁻¹ Y(ClO₄)₃ solution in D₂O from 3000 – 4000 cm⁻¹. The dominating O-H band at 3563 cm⁻¹ is due to the decoupled O-H oscillators, HDO/D₂O, weakly H-bonded to ClO₄⁻. In a concentrated Y(ClO₄)₃ solution the O-H⋯ClO₄⁻ band appears at 3538 cm⁻¹ (Figure S2).

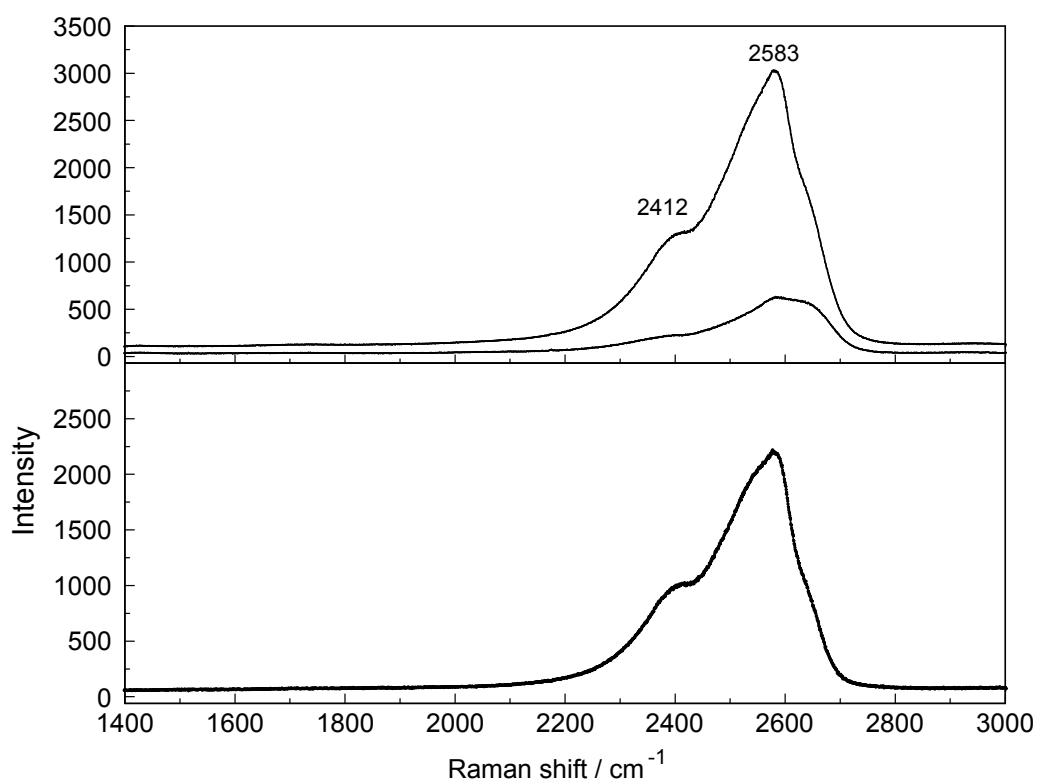


Figure S4. The O-D stretching region of heavy water from 1400 – 3000 cm⁻¹ of a 2.300 mol L⁻¹ Y(ClO₄)₃ solution in D₂O. The dominating O-D band at 2583 cm⁻¹ is due to the O-D oscillators weakly D-bonded to ClO₄⁻. Only one band component of the heavy water at 2412 cm⁻¹ appears while the component which normally appears at 2500 cm⁻¹ is almost completely overlapped by the strong band at 2583 cm⁻¹.

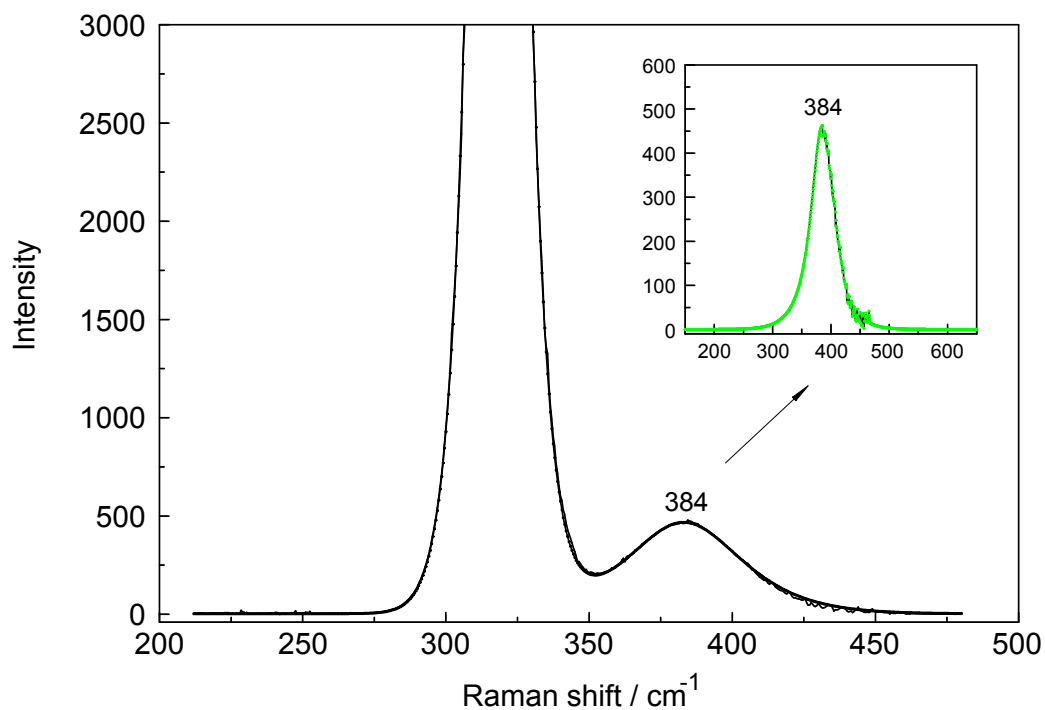


Figure S5. The isotropic Raman spectrum of a 1.10 molL⁻¹ Y(CF₃SO₃)₃ solution in the wavenumber range from 212 – 460 cm⁻¹ and the sum curve of the fit. The inset shows the result of the difference spectrum of the Y(CF₃SO₃)₃ spectrum from which the spectrum of CF₃SO₃⁻(aq) has been subtracted. The band at 384 cm⁻¹ is assigned to the YO₈ breathing mode.

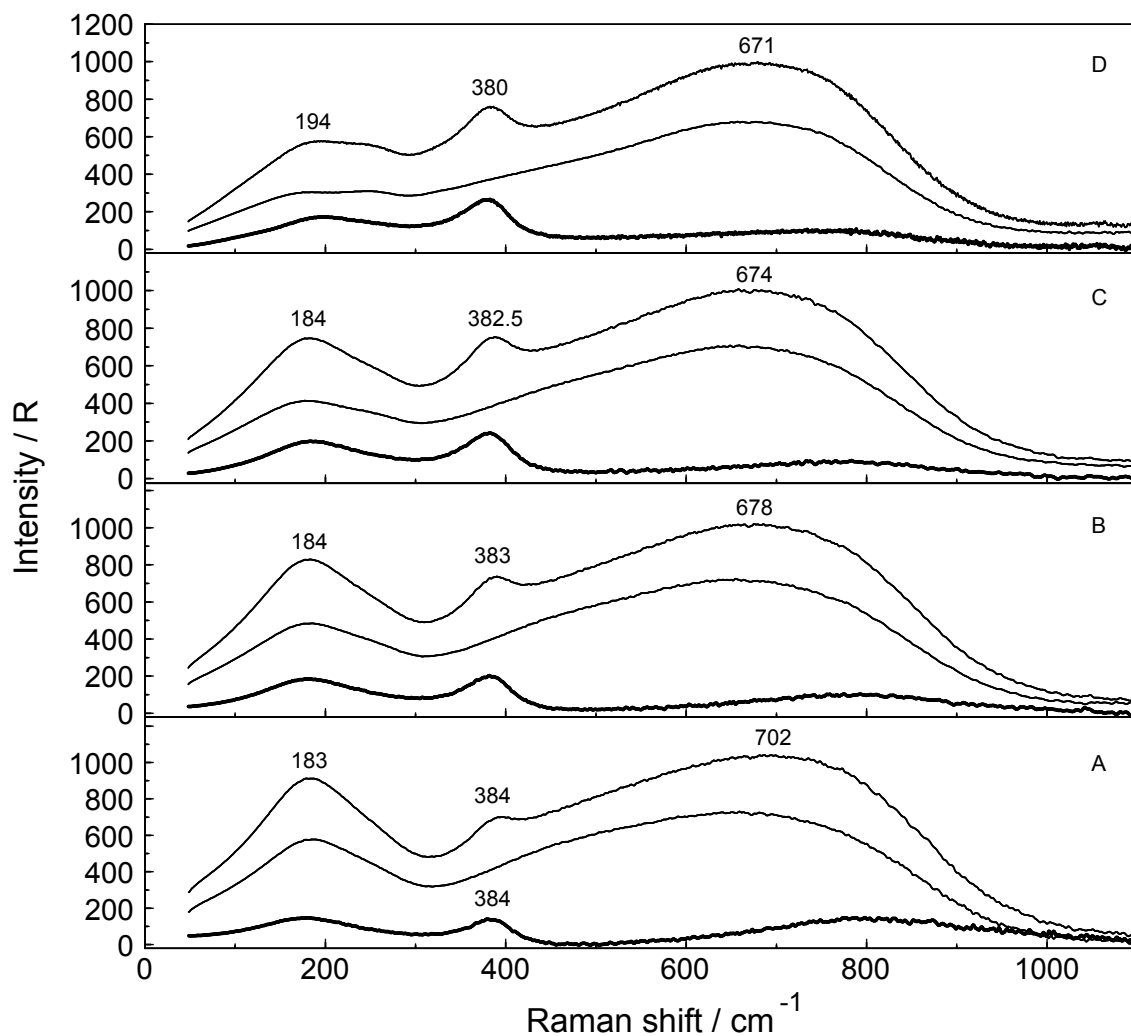


Figure S6. Raman scattering profiles (polarized, depolarized and isotropic (darker line) scattering orientations) of four YCl_3 solutions. From bottom to top: (A) $0.479 \text{ mol}\cdot\text{L}^{-1}$; (B) $0.803 \text{ mol}\cdot\text{L}^{-1}$; (C) $1.01 \text{ mol}\cdot\text{L}^{-1}$ and (D) $2.378 \text{ mol}\cdot\text{L}^{-1}$. The bands of the solute water are the restricted translation and the librational bands at $183\text{-}194 \text{ cm}^{-1}$ and $703 - 671 \text{ cm}^{-1}$.

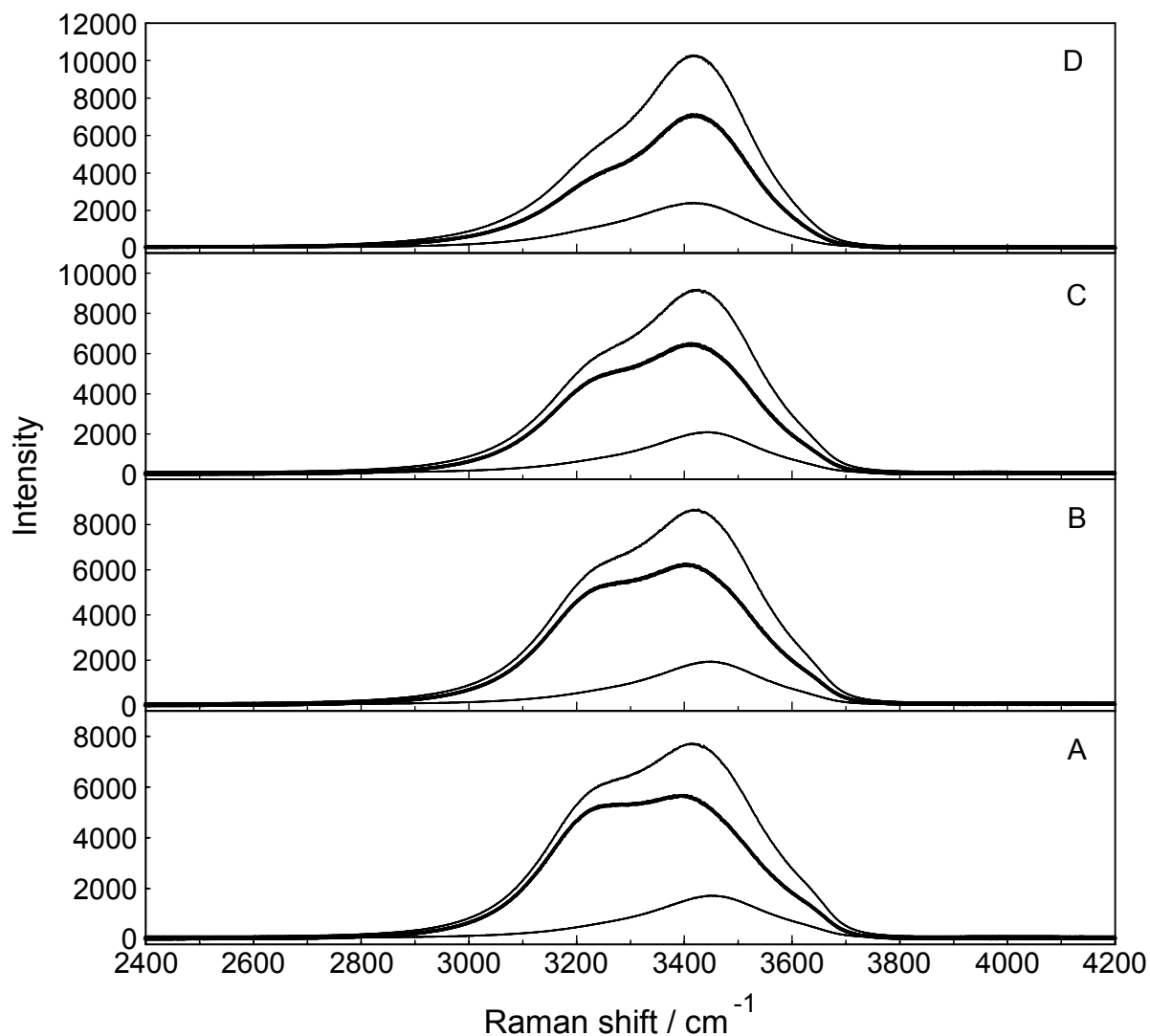


Figure S7. Raman scattering profiles (polarized, depolarized and isotropic (darker line) scattering orientations) of four YCl_3 solutions. From bottom to top: (A) $0.479 \text{ mol}\cdot\text{L}^{-1}$; (B) $0.803 \text{ mol}\cdot\text{L}^{-1}$; (C) $1.01 \text{ mol}\cdot\text{L}^{-1}$ and (D) $2.378 \text{ mol}\cdot\text{L}^{-1}$. Shown are the two water band components of the O-H stretching profile. The component bands for the O-H stretching profile of neat water are 3225 and 3405 cm^{-1} and a shoulder at 3630 cm^{-1} . The peak positions shift slightly to higher wavenumbers and for the $2.378 \text{ mol}\cdot\text{L}^{-1} \text{YCl}_3$ solution the band positions peak at 3220 cm^{-1} , 3425 cm^{-1} and a small shoulder at $3595\text{-}3625 \text{ cm}^{-1}$.

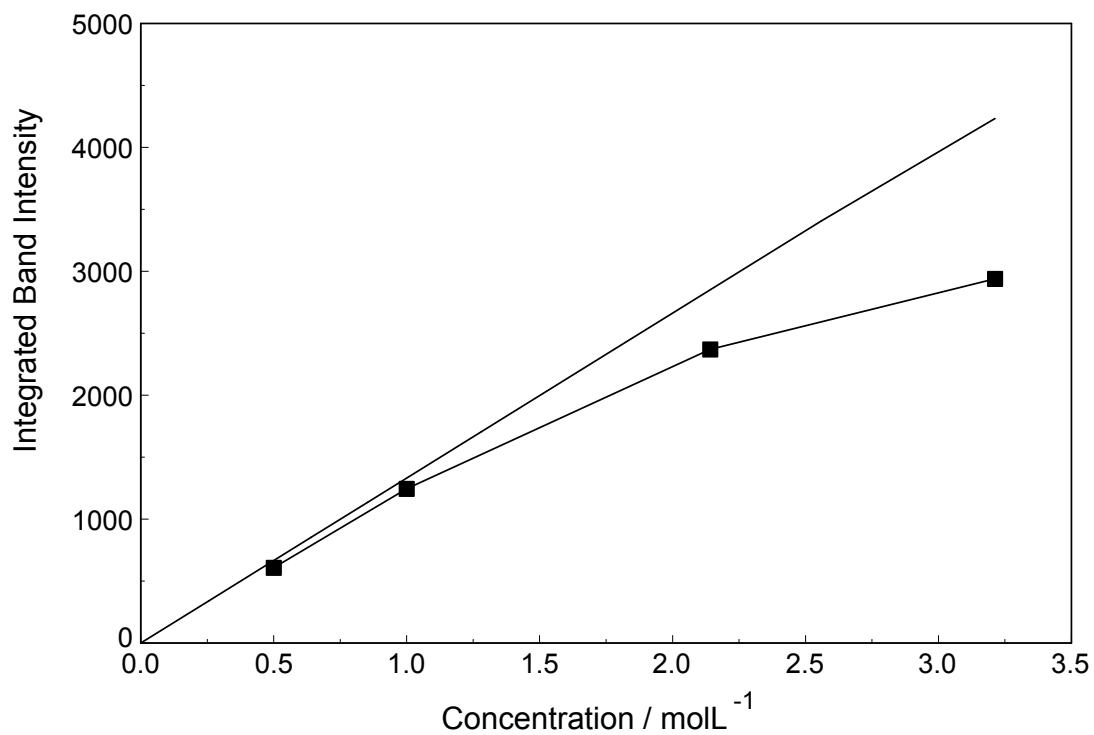


Figure S8. Quantitative Raman results: Integrated band intensities of the $\nu_1\text{YO}_8$ band versus stoichiometric concentration of four YCl_3 solutions (black squares) and the curve of the band intensity of $\nu_1\text{YO}_8$ as a function of concentration in $\text{Y}(\text{ClO}_4)_3(\text{aq})$.

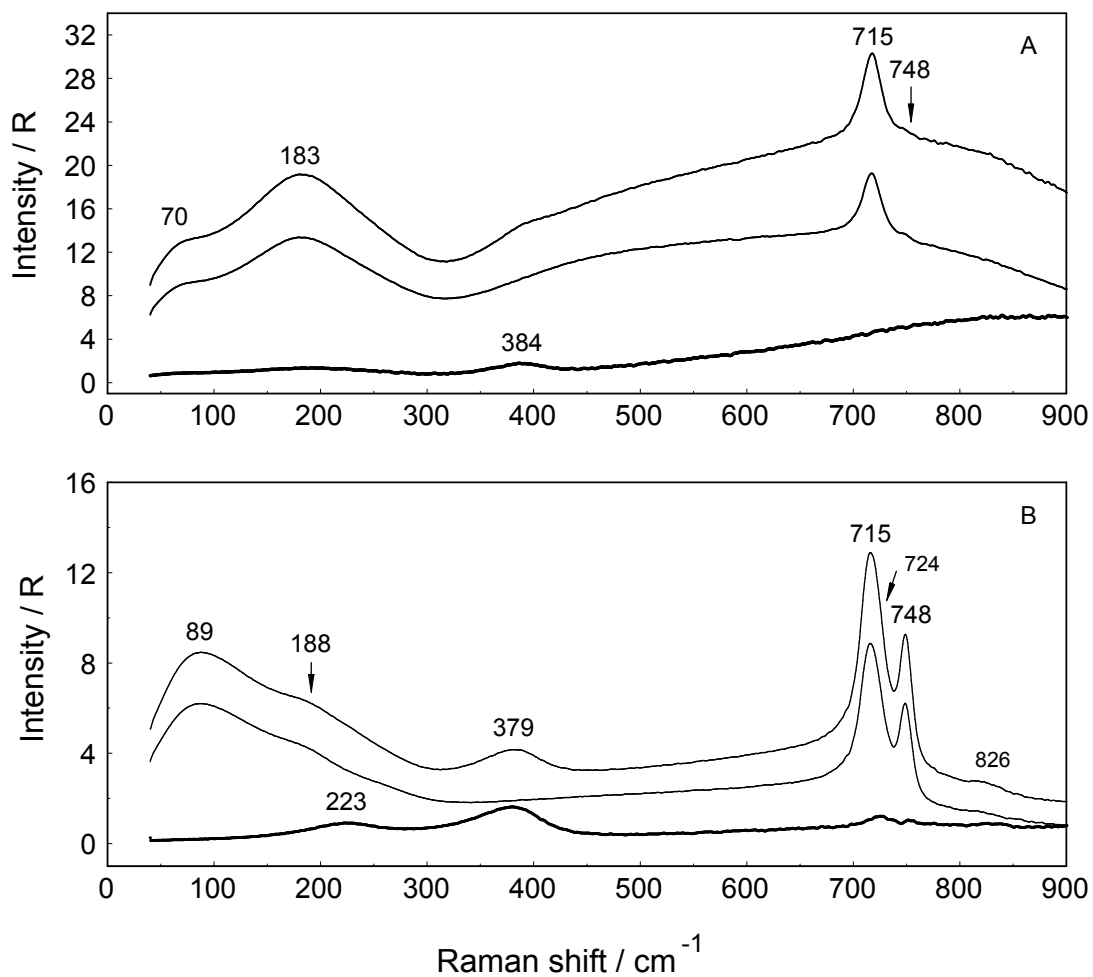


Figure S9. Raman spectra (R- format, all three scattering contributions): (A) a dilute solution at 0.198 mol·L⁻¹ Y(NO₃)₃ and (B) a concentrated solution at 2.035 mol·L⁻¹ in the frequency range from 40 - 900 cm⁻¹. Note the very weak band at 826 cm⁻¹ in panel (B) which is due to the normally infrared active mode, $\nu_2(a_2'')$.

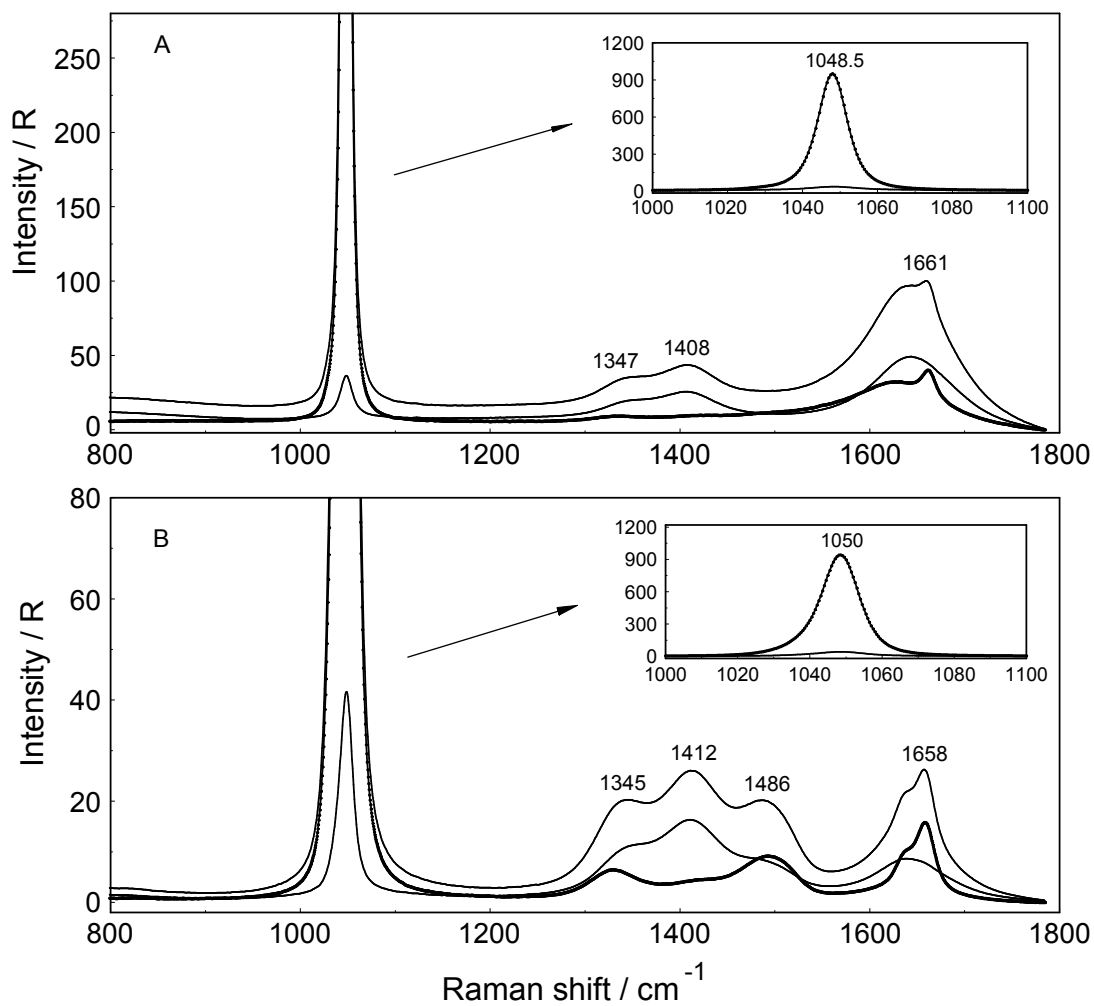


Figure S10. Raman spectra (R- format, all three scattering contributions) of A) dilute $\text{Y}(\text{NO}_3)_3$ solution at $0.198 \text{ mol}\cdot\text{L}^{-1}$ and B) of a $2.035 \text{ mol}\cdot\text{L}^{-1}$ solution at from $800 - 1800 \text{ cm}^{-1}$. The insets show the symmetric N-O stretching band in more detail (isotropic scattering and anisotropic scattering).